Magneto-Optical Investigation of the Broad Spin-Allowed Bands in the Metal–Metal-Bonded Complexes $Mo_2X_9^{3-}$ (X = Cl, Br)

Robert Stranger,*,† Grainne Moran,‡ Elmars Krausz,§ and Greg Medley†

Department of Chemistry, The University of Queensland, St. Lucia, QLD 4072, Australia, Department of Analytical Chemistry, University of New South Wales, Kensington, NSW 2033, Australia, and Research School of Chemistry, Australian National University, Canberra, ACT 2601, Australia

Received November 4, 1992•

The broad spin-allowed bands observed between 16 000 and 25 000 cm^{-1} in $Cs_3Mo_2X_9$ (X = Cl, Br) have been investigated by low-temperature single-crystal absorption and MCD spectroscopy. Using the exchange-coupled pair model, it is shown that these bands can be assigned to singly-excited pair states which involve trigonal $t_{2e} \rightarrow e$ single-ion excitation. Weaker, sharper features are also observed which are attributed to doubly-excited pair states arising from intraconfigurational transitions (spin-flips) within the t_{2e} single-ion orbitals. The spectral features are successfully modeled as a function of the Racah B and C parameters, the splitting between the trigonal t_{2e} and e single-ion orbitals, and the metal–metal π exchange interaction. From the analysis, the metal–metal π interaction in the bromide complex is shown to be weaker than that of the chloride complex. Spin-polarized, transition-state calculations using the SCF–Xα–SW method were carried out on $Cs_3Mo_2Cl_9$. Although the spin-singlet $\sigma(Mo_2) \rightarrow \sigma^*(Mo_2)$ transition is calculated around 21 000 cm^{-1} and is electric-dipole allowed, the low intensity ($\epsilon_{max} < 130$) in this region indicates that this transition lies to higher energy, above 27 000 cm^{-1}.

Introduction

In a number of reports,[1-3] we have examined in detail the electronic spectrum of the metal–metal-bonded dimer $Cs_3Mo_2Cl_9$ and shown that the exchange-coupled pair model provides a satisfying explanation for the observed band structure. Initially, the sharp multiplet structure observed below 16 000 cm^{-1} (see Figure 1 in ref 1) was assigned using the exchange-coupled pair model involving the trigonal $(t_{2g}^3)_a(t_{2g}^3)_b$ pair configuration (a and b refer to the two single-ion centers), incorporating both metal–metal σ and π exchange interactions parametrized by J_σ and J_π, respectively. This configuration comprises singly- and doubly-excited pair states derived from the $^4A_{2g}$, ^2E_g, $^2T_{1g}$, and $^2T_{2g}$ d^3 single-ion states. From the spectral analysis, the metal–metal σ interaction was shown to be quite strong ($J_\sigma = 20000 \pm 5000$ cm^{-1}) and the pair states converging to lowest energy corresponded to an effective $(t_{2e}^2)_a(t_{2e}^2)_b$ pair configuration in which the trigonal t_{2z} single-ion orbitals and accompanying electrons are essentially "factored out" energetically due to their participation in strong metal–metal σ bonding.

More recently, the theoretical model was extended to include the single-ion e_g orbitals as the exchange-coupled pair model involving the $(t_{2g}^3)_a(t_{2g}^3)_b$ configuration is only valid for small J_π. In the extended model, all pair states arising from the $(t_{2e}^{2-n}e^n)_a(t_{2e}^{2-n}e^n)_b$ ($n = 0, 1, 2$) configurations were included. As a result, it was possible to account for the anomalously low orbital g values found for the lowest lying pair multiplets around 8000 cm^{-1} in terms of extensive mixing of the trigonal t_{2e} and e single-ion orbitals by the metal–metal π interaction, $J_\pi = 7000 \pm 1000$ cm^{-1}. As noted previously,[4] J_π is defined in terms of cubic orbitals, but if trigonally-adapted t_{2g} orbitals are used, the metal–metal π interaction is significantly smaller, only $^1/_{18}$th of the value of J_π.

Calculations using the extended model above indicated that a large number of pair states involving single-ion $t_{2e} \rightarrow e$ excitation were predicted to lie between 16 000 and 25 000 cm^{-1} and, therefore, may account for the broad spin-allowed bands previously observed above 16 000 cm^{-1} in the absorption spectra of $Mo_2X_9^{3-}$ (X = Cl, Br) complexes.[5,6] Because of the close resemblance to monomeric MoX_6^{3-} (X = Cl, Br) spectra, these bands have been attributed to d^3 single-ion excitations and, more recently, to transitions involving metal–metal-based molecular orbitals.[7] However, assignment of these bands, as well as the multiplet structure observed below 16 000 cm^{-1}, on the basis of one-electron molecular-orbital excitations is not justified due to the extensive configuration interaction.

As a result of the relatively weak metal–metal bonding in $Cs_3Mo_2Cl_9$, the multiplet energies arising from the trigonal t_{2e} and e_g single-ion orbitals will be largely determined by electron repulsion and cubic field effects. Consequently, the exchange-coupled pair model is likely to be far more useful in describing the multiplet structure than any molecular-orbital based model. In order to test the validity of the exchange-coupled pair model in this region, we now report the low-temperature, magneto-optical study of the broad spin-allowed bands above 16 000 cm^{-1} in single-crystal $Cs_3Mo_2Cl_9$ and $Cs_3Mo_2Br_9$.

Experimental Section

Crystals of $Cs_3Mo_2X_9$ (X = Cl, Br) were grown from their powders by the Bridgeman method and sublimation. Thin axial plates suitable for MCD measurements were obtained by grinding and polishing sections cut from the Bridgeman samples. Small sublimed crystals less than 100 μm thick were used to measure the orthoaxial spectra. The apparatus used to measure low-temperature, single-crystal absorption and MCD

† The University of Queensland.
‡ University of New South Wales.
§ Australian National University.
• Abstract published in *Advance ACS Abstracts*, September 1, 1993.

(1) Dubicki, L.; Krausz, E.; Stranger, R.; Smith, P. W.; Tanabe, Y. *Inorg. Chem.* **1987**, *26*, 2247.
(2) Stranger, R. *Chem. Phys. Lett.* **1989**, *157*, 472.
(3) Stranger, R.; Moran, G.; Krausz, E.; Dubicki, L.; Güdel, H.; Furer, N. *Inorg. Chem.* **1992**, *31*, 2860.
(4) Stranger, R. *Inorg. Chem.* **1990**, *29*, 5231.
(5) Smith, P. W.; Wedd, A. G. *J. Chem. Soc. A* **1970**, 2447.
(6) Nguen Hyu Chi, Zelentsov, V. V.; Subbotina, N. A.; Spitsyn, V. I.; Fal'kengof, A. T. *Russ. J. Inorg. Chem. (Engl. Transl.)* **1972**, *17*, 1715.
(7) Trogler, W. C. *Inorg. Chem.* **1980**, *19*, 697.

0020-1669/93/1332-4555$04.00/0

spectra has been described in detail elsewhere.[8] SCF–Xα–SW calculations were performed using a modified version of the XASW program package written by Cook and Case.[11]

Results and Discussion

Theory. The multiplet structure of the $t_{2e}^2(^3A_2 + {}^1E + {}^1A_1)$, $t_{2e}^1e^1(^3A_1 + {}^3A_2 + {}^3E + {}^1A_1 + {}^1A_2 + {}^1E)$, and $e^2(^3A_2 + {}^1E + {}^1A_1)$ single-ion configurations for trigonal C_{3v} symmetry has been previously described.[4] Since the spin-allowed $t_{2e} \rightarrow e$ excitations should have large electric dipole intensity, only pair states derived from the single-ion spin-triplet states need be considered. The diagonal energies of these spin-triplet states with respect to the $^3A_2$ ground state are given by[4]

$$E(^3A_1) = \Delta - 3B$$

$$E(^3E) = \Delta + 3B$$

$$E(^3A_2) = \Delta + 9B$$

where Δ is the separation of the trigonal t_{2e} and e orbitals (of the order of $10Dq$ in the octahedral limit) and B is the Racah electron repulsion parameter. A recent optical study[8] of $MoCl_6^{3-}$ found $Dq = 1880$ cm^{-1} and $B = 490$ cm^{-1}. Therefore, on the basis of the above diagonal energies, one predicts the $t_{2e}^1e^1$ multiplets to lie between 17 000 and 24 000 cm^{-1}, and this is in reasonable agreement with the experimental spectrum as broad bands have been reported between 19 000 and 24 000 cm^{-1} for the absorption spectrum of $Mo_2Cl_9^{3-}$.[5,6]

In order to calculate the pair-state energies, it is necessary to diagonalize the single-ion and exchange Hamiltonians[4] for the $(t_{2e}^{2-n}e^n)_a(t_{2e}^{2-n}e^n)_b$ (n = 0, 1, 2) pair configurations. The appropriate D_{3h} pair basis functions can be constructed from

$$|\pm S_a\Gamma_aS_b'\Gamma_b'S\Gamma M\gamma\rangle = (1/\sqrt{2})(|S_a\Gamma_aS_b'\Gamma_b'S\Gamma M\gamma\rangle \pm |S_a'\Gamma_a'S_b\Gamma_bS\Gamma M\gamma\rangle)$$

where the ± sign refers to the symmetric and antisymmetric combination of C_{3v} pair basis functions given by

$$|n_aS_a\Gamma_an_b'S_b'S\Gamma M\gamma\rangle = \sum_{\substack{M_aM_b'\\ \gamma_a\gamma_b'}} (-1)^{S_a-S_b'+M}(2S+1)^{1/2}[\lambda(\Gamma)]^{1/2}\begin{pmatrix} S_a & S_b' & S \\ M_a & M_b' & M \end{pmatrix} \times V\begin{pmatrix} \Gamma_a & \Gamma_b' & \Gamma \\ \gamma_a & \gamma_b' & \gamma \end{pmatrix}|n_aS_a\Gamma_aM_a\gamma_a\rangle|n_b'S_b'\Gamma_b'M_b'\gamma_b'\rangle$$

Here n_a, S_a, and Γ_a refer to the single-ion configuration, spin, and orbital representation on center a (similarly for center b), respectively, while S, Γ, M, and γ refer to the total pair spin, orbital representation, magnetic-spin, and magnetic-orbital components, respectively. The vector coupling coefficient for spin angular momentum corresponds to Wigner's $3j$ coefficient,[18] while the point group coupling coefficient is Griffith's real trigonal V coefficient.[18,19]

In the kinetic exchange approximation where intercenter electron repulsion terms are neglected, the effective exchange Hamiltonian can be written as[4]

$$H_{ex} = 1/2 \sum_{\substack{a(\alpha\alpha')\\ b(\beta\beta')}} J(\alpha\alpha',\beta\beta')[-n_a(\alpha\alpha')n_b(\beta\beta') - 4S_a(\alpha\alpha')S_b(\beta\beta') + \delta(\beta\beta')n_a(\alpha\alpha') + \delta(\alpha\alpha')n_b(\beta\beta')]\delta(\alpha\beta')\delta(\beta\alpha')$$

where the localized orbitals $\alpha\alpha'$ and $\beta\beta'$ belong to metal centers a and b, respectively, and sum over both the t_{2e} and e single-ion orbitals. The generalized occupation number $n(\alpha\alpha')$, spin-operator $S(\alpha\alpha')$, and kinetic exchange parameter $J(\alpha\alpha',\beta\beta')$ are given by

$$n(\alpha\alpha') = \sum_\sigma a_{\alpha\sigma}^\dagger a_{\alpha'\sigma}$$

$$S(\alpha\alpha') = \sum_{\sigma\sigma'} \langle\sigma|S|\sigma'\rangle a_{\alpha\sigma}^\dagger a_{\alpha'\sigma'}$$

$$J(\alpha\alpha',\beta\beta') = -2h(\alpha\beta')h(\beta\alpha')/U$$

where $a_{\alpha\sigma}^\dagger$ and $a_{\alpha\sigma}$ are the creation and annihilation operators acting on spin orbitals in the second quantization scheme and $h(\alpha\beta)$ and U are the one-electron transfer integral and transfer energy, respectively. In the kinetic exchange approximation, if the metal–metal δ interaction is neglected, the various exchange parameters $J(\alpha\alpha',\beta\beta')$ can be expressed solely in terms of J_π, where

$$J_\pi = 4h_\pi^2/U$$

and h_π is the transfer integral involving either the xz or yz cubic orbitals quantized down the trigonal axis of the dimer.

The matrix elements of H_{ex} can be evaluated using the expressions given previously.[4] The single-ion matrix elements involving the electrostatic interaction and cubic ligand-field splitting have also been tabulated.[4] For simplicity, spin–orbit coupling effects are neglected since J_π is around an order of magnitude larger than $\zeta(Mo^{3+})$. Therefore, the analysis of the pair spectra of $Cs_3Mo_2X_9$ (X = Cl, Br) using the exchange-coupled pair model involves the fitting of four parameters, namely the Racah B and C electron repulsion parameters, the cubic-field splitting parameter Δ corresponding to the separation of the trigonal t_{2e} and e single-ion orbitals, and J_π, the metal–metal π exchange-interaction parameter. In the discussion to follow, we designate the multiplets arising from the various pair states using the notation $S\Gamma(S_a\Gamma_aS_b\Gamma_b)$ where $S\Gamma$ denotes the D_{3h} pair state multiplet and $S_a\Gamma_a$ and $S_b\Gamma_b$ refer to the single-ion states on metal centers a and b, respectively.

In order to obtain some indication of the pair states likely to occur between 16 000 and 25 000 cm^{-1}, calculations were performed with the single-ion parameters set to B = 395, C = 1460, and Δ = 20 800 cm^{-1}, corresponding to the best-fit values for the lower lying pair states (below 16 000 cm^{-1}), which have been well characterized in past studies.[1-3] The C/B ratio was maintained at 3.7 corresponding to the value found from a recent detailed spectroscopic analysis[8] of $MoCl_6^{3+}$ doped in the cubic host material Cs_2NaYCl_6. The resulting energies of the spin-

(8) (a) Stranger, R.; Moran, G.; Krausz, E.; Güdel, H.; Furer, N. *Mol. Phys.* **1990**, *69*, 11. (b) Krausz, E. *Aust. J. Chem.* **1993**, *46*, 1041.
(9) Piepho, S. B.; Schatz, P. N. *Group Theory in Spectroscopy with Applications to Magnetic Circular Dichroism*; Wiley and Sons: New York, 1983.
(10) Slater, J. C. *Quantum Theory of Molecules and Solids*; McGraw-Hill: New York, 1974; Vol. 4.
(11) Cook, M.; Case, D. A. XASW-A Fortran Program Package for Atomic X-Alpha and Molecular Multiple-Scattering X-Alpha Electronic Structure Calculations, Version 2. QCPE Program 465, 1982.
(12) (a) Levenson, R. A.; Gray, H. B. *J. Am. Chem. Soc.* **1975**, *97*, 6042. (b) Miskowski, V. M.; Smith, T. P.; Loehr, T. M.; Gray, H. B. *J. Am. Chem. Soc.* **1985**, *107*, 7925. (c) Miskowski, V. M.; Schaefer, W. P.; Sadeghi, B.; Santarsiero, B. D.; Gray, H. B. *Inorg. Chem.* **1984**, *23*, 1154. (d) Isci, H.; Mason, W. R. *Inorg. Chem.* **1985**, 1761. (e) Newman, R. A.; Martin, D. S.; Dallinger, R. F.; Woodruff, W. H.; Stiegman, A. E.; Che, C.-M.; Schaefer, W. P.; Miskowski, V. M.; Gray, H. B. *Inorg. Chem.* **1991**, *30*, 4647. (f) Gökagac, G.; Isci, H.; Mason, W. R. *Inorg. Chem.* **1992**, *31*, 2184.
(13) Hopkins, M. D.; Gray, H. B.; Miskowski, V. M. *Polyhedron* **1987**, *6*, 705.
(14) Stranger, R.; Smith, P. W.; Grey, I. E. *Inorg. Chem.* **1989**, *28*, 1271.
(15) Saillant, R.; Jackson, R. B.; Streib, W. E.; Folting, K.; Wentworth, R. A. D. *Inorg. Chem.* **1971**, *10*, 1453.
(16) Güdel, H. U.; Dubicki, L. *Chem. Phys.* **1974**, *6*, 272.
(17) Noodleman, L.; Norman, J. G. *J. Chem. Phys.* **1979**, *70*, 4903.
(18) Silver, B. L. *Irreducible Tensor Methods*; Academic Press: New York, 1976.
(19) Griffith, J. S. *The Irreducible Tensor Method for Molecular Symmetry Groups*; Prentice Hall: Englewood Cliffs, NJ, 1962.

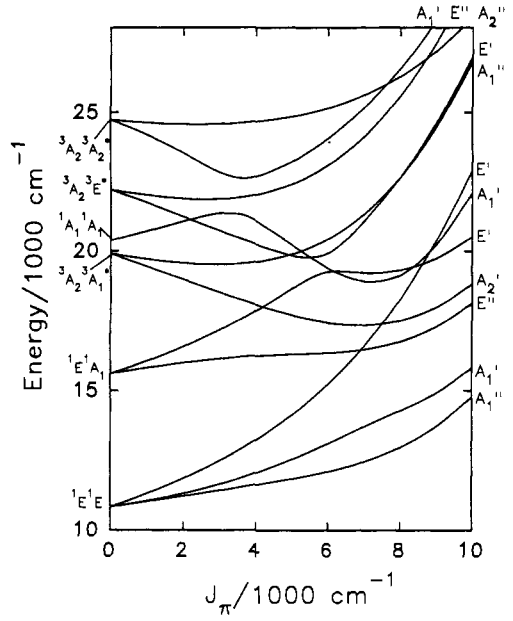

Figure 1. Calculated energy levels for the $(t_{2e}^{2-n}e^n)_a(t_{2e}^{2-n}e^n)_b$ (n = 0, 1, 2) pair configurations as a function of J_π. Single-ion parameters are set to B = 395, C = 1460, and Δ = 20 800 cm^{-1}. Only the S = 0 doubly-excited pair states belonging to the $(t_{2e}^2)_a(t_{2e}^2)_b$ configuration, and the S = 0 singly-excited pair states belonging to the $(t_{2e}^2)_a(t_{2e}^1e^1)_b$ configuration (denoted by an asterisk) are shown. Pair states are labeled on the left-hand side of the figure, while the resulting D_{3h} multiplets are labeled on the right-hand side.

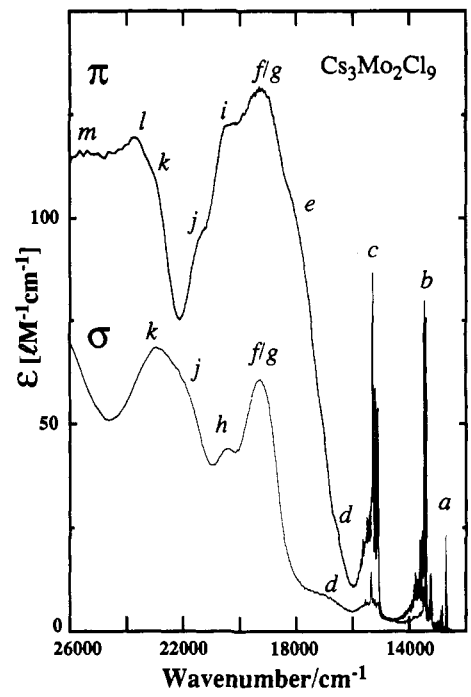

Figure 2. Polarized absorption spectrum of a 70 μm thick single crystal of $Cs_3Mo_2Cl_9$ at 5 K. The π and σ spectra refer to light polarized along and perpendicular to the metal–metal axis of the dimer, respectively. (See Table I for the labeling of bands.)

singlet pair states relative to the $^1A_1'(^3A_2{}^3A_2)$ ground state are plotted as a function of J_π in Figure 1. Pair states involving the single-ion e^2 configuration are not shown as they occur to higher energy, well above the region of spectroscopic interest.[4] For J_π ~ 6200 cm^{-1}, corresponding to the best fit for the lower lying pair multiplets, nine spin-singlet pair states fall within the specified range as can be seen from Figure 1. If one includes spin-triplet pair states, the overall density of states in this region is quite high, approximately 30 pair states in all. However, only the spin-singlet pair states are considered in this analysis as they should dominate in intensity.

$Cs_3Mo_2Cl_9$. The single-crystal, orthoaxial (σ and π polarizations) absorption spectrum of $Cs_3Mo_2Cl_9$ at 5 K is shown in Figure 2, while the 1.8 K axial absorption and MCD (5 T) spectra are shown in Figure 3. The MCD spectrum was not reliable above 22 000 cm^{-1} because of uncertainty in the baseline. Broad bands are observed at approximately 17 000 (d), 18 000 (e), 19 250 (f/g), 20 500 (h/i), 21 500 (j), 23 000 (k), 23 700 (l), and 25 500 (m) cm^{-1}. The sharp structure observed between 12 500 and 16 000 cm^{-1} (bands a–c) has previously been assigned to the $^1E^1E$ double excitation arising from the $(t_{2e}^2)_a(t_{2e}^2)_b$ pair configuration.[1,2] These bands are strongly π polarized with ϵ_{max} ~ 80 greater than that for the broad spin-allowed bands above 16 000 cm^{-1} in σ polarization. Furthermore, the π intensity for these bands has been shown to be vibronically induced.[1,2] For the broad bands above 16 000 cm^{-1}, the π polarization is about twice the intensity of the σ polarization with ϵ_{max} values as large as 130.

From Figure 1 there is only one π polarized, spin-allowed pair state below 30 000 cm^{-1}, corresponding to $^1A_2''(^3A_2{}^3A_2{}^*)$ (an asterisk is used to denote states arising from the single-ion $t_{2e}^1e^1$ configuration). Therefore, it must be concluded that the bulk of π intensity observed between 12 000 and 25 000 cm^{-1} is vibronically induced and, consequently, the polarization behavior of the bands cannot be relied on for assignment purposes. Unfortunately, the temperature dependence of these bands is difficult to assess, due to their dramatic sharpening on cooling, and therefore cannot be used as a reliable indication of vibronic intensity. The π

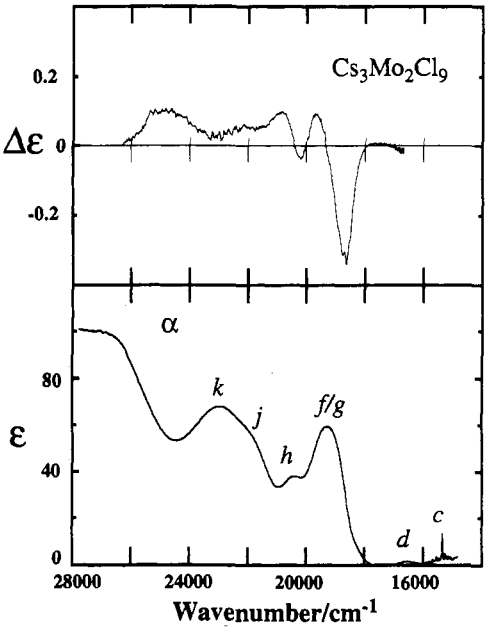

Figure 3. Axial absorption and MCD spectra (5 T) of $Cs_3Mo_2Cl_9$ at 1.8 K. Because of baseline uncertainty, the MCD spectrum is not reliable above 22 000 cm^{-1}. (See Table I for the labeling of bands.)

intensity most likely arises from vibronic mixing with the z-polarized $\sigma(Mo_2) \rightarrow \sigma^*(Mo_2)$ transition or $Mo^{III}Mo^{III} \rightarrow Mo^{II}Mo^{IV}$ charge-transfer transition. A similar situation occurs in basic rhodo $[(NH_3)_5Cr{-}O{-}Cr(NH_3)_5]^{4+}$, where the intense z-polarized bands associated with the double excitations were shown to arise from a vibronically induced exchange mechanism, the intensity being borrowed from the higher energy π polarized Cr $\leftrightarrow$ Cr charge-transfer transition.[16] Strong, vibronically induced π intensity also occurs in the spectrum of the $Mn_2(CO)_{10}$ dimer complex and was attributed to mixing with the intense $\sigma(M_2) \rightarrow \sigma^*(M_2)$ transition to higher energy.[12a,b]

The MCD spectrum (Figure 3) displays a prominent positive A term associated with the broad band (f) centered at 19 250

cm^{-1} and another weaker positive A term corresponding to the weak band (h) at 20 500 cm^{-1}. The asymmetric nature of both A terms partly results from their overlap but it is also possible that a negative B term is contributing to this band region. The weak band (d) at ~17 000 cm^{-1} exhibits very weak MCD in the form of a positive A term. The A terms observed in the MCD spectrum are associated with transitions from the $^1A_1'(^3A_2{}^3A_2)$ ground state to either $^1E'$ or $^1E''$ excited pair states, though in the latter case the intensity will be vibronically induced.

For J_π = 6200 cm^{-1}, the doubly-excited $^1E''(^1E^1A_1)$ pair state is calculated to lie at ~16 500 cm^{-1}. This transition is expected to be weak since it is electric-dipole forbidden. It should also be quite sharp as it is an intraconfigurational transition arising from the $(t_{2e}{}^2)_a(t_{2e}{}^2)_b$ pair configuration.[4] However, for $J_\pi \sim$ 6200 cm^{-1}, this state is significantly mixed with the singly-excited $^1E''$-$(^3A_2{}^3E^*)$ pair state which involves $t_{2e} \rightarrow e$ excitation, and this may result in a significant broadening of the $^1E''(^1E^1A_1)$ state. The transition to the $^1E''(^1E^1A_1)$ state is expected to exhibit MCD on the basis of its diagonal orbital moment of $+2k$ determined previously,[4] and this is consistent with the weak positive A term associated with the weak, broad absorption (d) at ~17 000 cm^{-1} seen in both the axial and σ spectra (Figures 2 and 3). The positive sign of the A term implies coupling of the $^1E''$ origin with either A_1'' or A_2'' vibrations. This transition is also seen in π polarization (Figure 2) in the form of fine structure at ~17 000 cm^{-1} superimposed on the broad, relatively intense shoulder (e) at ~18 000 cm^{-1}.

The transition to $^1A_2'(^3A_2{}^3A_1{}^*)$, calculated at ~17 350 cm^{-1}, is predicted to be the lowest lying spin-allowed pair state involving $t_{2e} \rightarrow e$ excitation. On the basis of position, the broad, relatively intense π polarized shoulder (e) at ~18 000 cm^{-1} is assigned to this pair state in which case the intensity must be induced through coupling with an A_1'' vibrational mode.

The $^1E'(^3A_2{}^3E^*)$ and $^1E'(^1E^1A_1)$ pair states are calculated to lie at approximately 19 300 and 20 250 cm^{-1}, respectively. Transitions to both states are electric dipole allowed in σ polarization. Again, although the $^1E'(^1E^1A_1)$ state arises from the $(t_{2e}{}^2)_a(t_{2e}{}^2)_b$ pair configuration, it should be relatively broad since it is strongly mixed with the $^1E'(^3A_2{}^3E^*)$ pair state for $J_\pi \sim$ 6200 cm^{-1}. The $^1E'(^3A_2{}^3E^*)$ and $^1E'(E^1A_1)$ pair states are both orbital doublets which are expected to exhibit positive A MCD terms due to their diagonal orbital moments of $+k'$ and $+2k$, respectively.[4] The sign of the observed MCD for the bands seen in axial and σ polarization at approximately 19 250 (f) and 20 500 (h) cm^{-1} is consistent with the $^1E'(^3A_2{}^3E^*)$ and $^1E'(^1E^1A_1)$ pair states, respectively.

On the assumption of a Gaussian band shape, the observed $(\Delta A/A)_{max}$ values for the $^1E''(^1E^1A_1)$, $^1E'(^3A_2{}^3E^*)$, and $^1E'(^1E^1A_1)$ pair states can be used to determine the experimental g-values which can then be compared with the theoretical values in order to verify the above assignments. The $(\Delta A/A)_{max}$ values are related to the MCD parameter ratio A_1/D_0 through the expression[9]

$$\left(\frac{\Delta A}{A}\right)_{max} = \frac{1.428\beta H}{\nu_{1/2}}\left(\frac{A_1}{D_0}\right)$$

where $\nu_{1/2}$ is the full width at half-height band parameter. For a nondegenerate groundstate, A_1 and D_0 are given by

$$A_1 = \sum_\lambda g_\lambda(|\langle A|m_{-1}|J\lambda\rangle|^2 - |\langle A|m_{+1}|J\lambda\rangle|^2)$$

$$D_0 = {}^1/_2\sum_\lambda(|\langle A|m_{-1}|J\lambda\rangle|^2 + |\langle A|m_{+1}|J\lambda\rangle|^2)$$

where A and J are the ground and excited states, λ's are the components of J, $m_{\pm1}$ is the electric-dipole operator, and $g_\lambda = \langle J\lambda|L_z + 2S_z|J\lambda\rangle$ is the excited-state g-value or Zeeman shift. Summing over the orbital components $\lambda = \pm1$ in the above expressions for A_1 and D_0 gives the simple relation

$$\frac{A_1}{D_0} = 2g$$

where g, the experimental g-value, can be compared to the theoretical value g_λ above.

From the observed $(\Delta A/A)_{max}$ values, experimental g-values of 1.4 ± 0.6, 0.8 ± 0.4, and 1.8 ± 0.5 are obtained for the MCD A terms associated with the bands observed at approximately 17 000 (d), 19 250 (f), and 20 500 (h) cm^{-1}, respectively. The uncertainty in the last two g-values arises from the asymmetric nature of the observed MCD A terms, whereas the uncertainty for the first g-value is due to the inherent weakness of both ΔA and A for the 17 000 (d) cm^{-1} band. Although the sign of the g-values is consistent with the proposed assignments, their magnitudes deviate from the theoretical g-values of $+2k$, $+k'$, and $+2k$ for the $^1E''(^1E^1A_1)$, $^1E'(^3A_2{}^3E^*)$, and $^1E'(^1E^1A_1)$ pair states, respectively, where the orbital reduction parameters k and k' are assumed to be ~1. However, the theoretical values ignore configuration interaction which has already been shown to be significant for these pair states. A calculation for J_π = 6200 cm^{-1} with $k = k' = 1$, which takes account of configuration interaction, results in g-values of approximately 1.2, 1.0, and 1.8 for the $^1E''(^1E^1A_1)$, $^1E'(^3A_2{}^3E^*)$, and $^1E'(^1E^1A_1)$ pair states, respectively, which are now in good agreement with the above experimental values.

The doubly-excited $^1A_1'(^1A_1{}^1A_1)$ and singly-excited $^1A_1''$-$(^3A_2{}^3A_1{}^*)$ pair states are calculated at approximately 19 350 and 20 600 cm^{-1}, with the former pair state being significantly mixed with $^1A_1'(^3A_2{}^3A_2{}^*)$ for J_π = 6200 cm^{-1}. On the basis of position, the shoulder (i) at ~20 500 cm^{-1} in π polarization is assigned to $^1A_1''(^3A_2{}^3A_1{}^*)$ but it is also possible that all or part of this band is due to $^1E'(^1E^1A_1)$ since from the MCD spectrum this state is associated with the weak 20 500 cm^{-1} band (h) observed in both the axial and σ polarized spectra. From the calculated position for $^1A_1'(^1A_1{}^1A_1)$, it is anticipated that this state will overlap with $^1E'(^3A_2{}^3E^*)$ and therefore contribute to the band intensity observed in both σ and π polarization at ~19 250 cm^{-1}.

Higher lying spin-singlet pair states are calculated at approximately 23 350, 24 450, and 25 300 cm^{-1} for the $^1E''(^3A_2{}^3E^*)$, $^1A_1'(^3A_2{}^3A_2{}^*)$, and $^1A_2''(^3A_2{}^3A_2{}^*)$ pair states, respectively. With the exception of $^1A_2''(^3A_2{}^3A_2{}^*)$, the remaining pair states are electric-dipole forbidden in both σ and π polarization and, therefore, any intensity will be vibronically induced. On the basis of calculated position, the band (k) observed at ~23 000 cm^{-1} in both σ and π polarization is assigned to the $^1E''(^3A_2{}^3E^*)$ pair state. This state should exhibit MCD, but since it was not possible to obtain reliable MCD above 22 000 cm^{-1}, this prediction cannot be tested. The π polarized bands at approximately 23 700 (l) and 25 500 (m) cm^{-1} are assigned to the $^1A_1'(^3A_2{}^3A_2{}^*)$ and $^1A_2''$-$(^3A_2{}^3A_2{}^*)$ pair states, respectively.

Weak shoulders are observed in both σ and π polarization between 21 000 and 22 000 cm^{-1}, and since no spin-singlet pair state transitions are calculated in this region, they are assigned to the spin-triplet $^3E''(^3A_2{}^3E^*)$ pair state calculated at ~21 850 cm^{-1}. This pair state comprises $A_1' + A_2' + E' + E''$ spin–orbit levels of which the transition to E' will be σ polarized. The observed and calculated energy levels for $Cs_3Mo_2Cl_9$ are given in Table I.

It is conceivable that part of the observed band structure between 16 000 and 27 000 cm^{-1} is due to $\sigma(Mo_2) \rightarrow \sigma^*(Mo_2)$ and $\sigma(Mo_2) \rightarrow \sigma^*(Mo\text{–}Cl)$ type molecular-orbital transitions.[7] Since the exchange-coupled pair model is unable to account for such transitions due to its inherent single-ion based formalism, we undertook spin-polarized, transition-state calculations on $Cs_3Mo_2Cl_9$ using the SCF–Xα–SW method.[10,11] From these calculations, the $\sigma(Mo_2) \rightarrow \sigma^*(Mo_2)$ spin-singlet transition, which should be π polarized, is predicted at approximately 21 000 cm^{-1}

Table I. Observed and Calculated Band Positions (cm^{-1}) and Assignments for the Polarized, Single-Crystal Absorption Spectra of $Cs_3Mo_2X_9$ (X = Cl, Br)

$Cs_3Mo_2Cl_9$		$Cs_3Mo_2Br_9$			
calc[a]	obs	calc[b]	obs	label	assgnt[c]
12 250	12 450	11 700	12 100	a	$^1A_1''(^1E^1E)$
13 350	13 150	12 750	12 700	b	$^1A_1'(^1E^1E)$
15 600	15 300	14 750	14 800	c	$^1E'(^1E^1E)$
16 500	17 000	15 750	16 000	d	$^1E''(^1E^1A_1)$
17 350	18 000	15 300	15 500	e	$^1A_2'(^3A_2{}^3A_1{}^*)$
19 300	19 250	17 400	17 500	f	$^1E'(^3A_2{}^3E^*)$
19 350	19 250	18 150	18 800	g	$^1A_1'(^1A_1{}^1A_1)$
20 250	20 500	19 250	19 200	h	$^1E'(^1E^1A_1)$
20 600	20 500	18 250	19 700	i	$^1A_1''(^3A_2{}^3A_1{}^*)$
21 850	21 500	19 550	19 700	j	$^3E''(^3A_2{}^3E^*)$
23 350	23 000	21 200	21 000	k	$^1E''(^3A_2{}^3E^*)$
24 450	23 700	23 500	*d*	l	$^1A_1'(^3A_2{}^3A_2{}^*)$
25 300	25 500	22 800	*d*	m	$^1A_2''(^3A_2{}^3A_2{}^*)$

[a] Calculated energies for B = 395, C = 1460, Δ = 20800, and J_π = 6200 cm^{-1}. [b] Calculated energies for B = 390, C = 1450, Δ = 18450, and J_π = 5350 cm^{-1}. [c] Assignments are given as D_{3h} multiplets with the associated pair state in parentheses. An asterix denotes a single-ion state arising from the $(t_{2e})^1(e)^1$ configuration. Only transitions to $E'(\sigma)$ and $A_2''(\pi)$ states are electric-dipole allowed. Observed intensity for all other states is vibronically induced. [d] Absorption spectrum not measured beyond 22 500 cm^{-1} for $Cs_3Mo_2Br_9$.

and with an oscillator strength approaching 1. However, below 27 000 cm^{-1} the maximum π intensity (ϵ_{max} = 130) is very low in comparison with other $\sigma(M_2) \rightarrow \sigma^*(M_2)$ transitions, where ϵ_{max} is around 2 orders of magnitude larger.[12] In fact, the observed intensity is similar to that for $\delta(M_2) \rightarrow \delta^*(M_2)$ transitions in d^4d^4 quadruple-bonded M_2L_8 complexes,[13] where SCF–Xα–SW calculations underestimate the transition energy by a factor of nearly 2. The discrepancy has been attributed to the large ionic dependence and metal-localized character associated with this transition due to the weakness of the metal–metal δ interaction.[13] In the case of the quadruple metal–metal-bonded complex $Mo_2Cl_8^{4-}$, the calculated $\delta(Mo_2) \rightarrow \delta^*(Mo_2)$ transition energy was dramatically improved using the Xα–VB valence bond model.[17] We are currently carrying out such calculations for $Cs_3Mo_2Cl_9$.

With regard to $Cs_3Mo_2Cl_9$, we have previously shown[14] that the t_{2z} electrons are not fully paired-off into a metal–metal σ bond, and although this will obviously result in greater ionic character and a lower transition intensity for the $^1A_1' \rightarrow {}^1A_2''$ ($\sigma \rightarrow \sigma^*$) transition, it is highly unlikely that ϵ_{max} could be as low as 130 for this type of transition. Other metal–metal σ bonded dimers exhibit very intense $\sigma \rightarrow \sigma^*$ transitions, with oscillator strengths approaching 1.[12b] It is therefore concluded that the $\sigma(Mo_2) \rightarrow \sigma^*(Mo_2)$ transition in $Cs_3Mo_2Cl_9$ lies above 27 000 cm^{-1}.

The $\sigma(Mo_2) \rightarrow \sigma^*$(Mo–Cl) spin singlet transitions are calculated to lie above 30 000 cm^{-1}, and this seems too high to be associated with the observed band structure between 21 000 and 25 000 cm^{-1}. The broad rising band seen in σ polarization above 25 000 cm^{-1} may in part be due to these transitions or the corresponding spin-triplet transitions.

$Cs_3Mo_2Br_9$. The detailed, low-temperature, polarized single-crystal absorption spectrum of $Cs_3Mo_2Br_9$ below 15 000 cm^{-1} will be reported in a later study.[20] Above 15 000 cm^{-1} the low-temperature, orthoaxial single-crystal absorption spectrum at 5 K, shown in Figure 4, bears some similarity to that of the chloride complex with relatively broad bands observed at 21 000 (k), 19 700 (i/j), 19 200 (h), 18 800 (g), 17 500 (f), and 15 500 (e) cm^{-1}. Weak, sharper features are superimposed on the latter broad π polarized band at approximately 16 000 (d) and 14 800 (c) cm^{-1} with corresponding absorptions also seen in σ polarization. Analogous to the chloride complex, the lower energy sharp

(20) Stranger, R.; Krausz, E.; Dubicki, L. To be published.

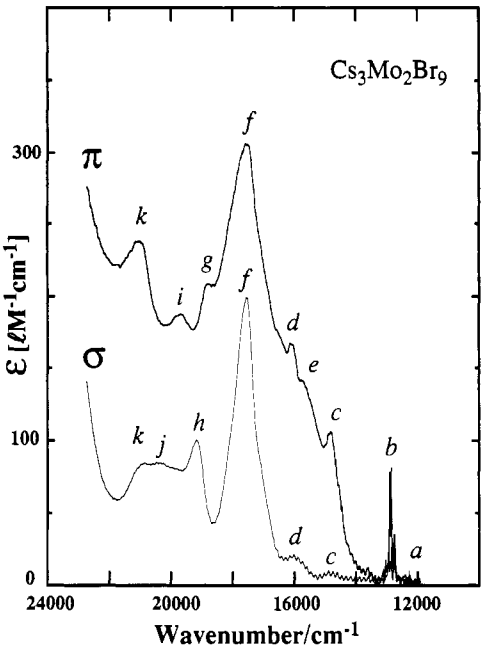

Figure 4. Polarized absorption spectrum of a 35 μm thick single crystal of $Cs_3Mo_2Br_9$ at 5 K. The π and σ spectra refer to light polarized along and perpendicular to the metal–metal axis of the dimer, respectively. Note that interference fringes are observed in σ polarization between 13 000 and 16 500 cm^{-1}. (See Table I for the labeling of bands.)

structure (bands a and b) can be assigned to the $^1E^1E$ double excited-pair state.[20]

On the basis of the above assignments for the chloride complex, the bands at 15 500 (e), 17 500 (f), 19 200 (h), and 21 000 (k) cm^{-1} are assigned to the $^1A_2'(^3A_2{}^3A_1{}^*)$, $^1E'(^3A_2{}^3E^*)$, $^1E'(^1E^1A_1)$, and $^1E''(^3A_2{}^3E^*)$ pair states, respectively. Likewise, the additional weak bands in π polarization at 18 800 (g) and 19 700 (i/j) cm^{-1} are assigned to the $^1A_1''(^3A_2{}^3A_1{}^*)$ and $^3E''(^3A_2{}^3E^*)$ pair states, while the weaker sharper features to lower energy at 16 000 (d) and 14 800 (c) cm^{-1}, indicative of doubly-excited pair transitions arising from the $(t_{2e}^2)_a(t_{2e}^2)_b$ configuration, are assigned to the $^1E''(^1E^1A_1)$ and $^1E'(^1E^1E)$ pair states, respectively. The $^1A_1'$-$(^1A_1{}^1A_1)$ pair state is calculated at ~18 150 cm^{-1}, very close to $^1A_1''(^3A_2{}^3A_2{}^*)$ and, therefore, possibly contributes intensity to the π polarized band (g) at ~18 800 cm^{-1}.

The sharp multiplet structure[20] below 15 000 cm^{-1} as well as the broad bands above 15 000 cm^{-1} can be best-fitted for the parameter values B = 390, C = 1450, Δ = 18 500, and $J_\pi \sim$ 5300 cm^{-1}. The observed and calculated energies for these parameter values are given in Table I. The smaller value of J_π for the bromide complex (cf. J_π = 6200 cm^{-1} for $Cs_3Mo_2Cl_9$) implies weaker metal–metal π bonding, and this is consistent with the increased metal–metal distance of 0.16 Å for the bromide complex.[15] That the Racah B and C parameters are almost the same as those found for the chloride complex is coincidental. The expected decrease in B and C due to covalency effects on replacing chloride with bromide is offset by a reduction in covalency due to reduced M–M σ and π bonding for the bromide complex. The 1000–2000-cm^{-1} shifts to lower energy observed for the broad bands above 15 000 cm^{-1} in $Cs_3Mo_2Br_9$ is largely due to the reduction in Δ whereas the smaller 500–1000-cm^{-1} shifts observed for the multiplet structure below 15 000 cm^{-1} is mainly due to a reduction in the metal–metal π-bonding for the bromide complex as evidenced by the smaller value of J_π.

Conclusion

The present analysis has shown that the broad spin-allowed bands observed between 16 000 and 25 000 cm^{-1} in $Cs_3Mo_2X_9$ (X = Cl, Br) can be assigned on the basis of the exchange-coupled pair model in which the single-ion trigonal t_{2z} orbitals have been

effectively "factored out" energetically due to strong metal–metal σ bonding. The majority of bands observed in this region are consistent with pair-state transitions which largely involve trigonal $t_{2e} \rightarrow e$ single-ion excitation, accounting for their broadness in relation to the sharp multiplet structure observed below 16 000 cm^{-1}.

The detailed analysis of the electronic spectrum of $Cs_3Mo_2Cl_9$ has clearly demonstrated that the exchange-coupled pair model is quite successful in describing, semiquantitatively, the electronic structure of polynuclear complexes exhibiting moderate to strong metal–metal bonding. However, it must be recognized that this model deals only with states arising from metal–metal interactions in which electrons are not fully paired off into metal–metal bonds. In this respect, the edge-shared M_2L_{10} bioctahedra complexes of Mo(III) and W(III) are likely candidates for the application of this model as they display metal–metal bond lengths, room-temperature paramagnetism, and electronic spectra similar to their face-shared M_2L_9 counterparts.[21-24]

Acknowledgment. R.S. gratefully acknowledges the financial support of the Australian Research Council.

(21) Cotton, F. A. *Polyhedron* **1987**, *6*, 667.
(22) Cotton, F. A.; Diebold, M. P.; O'Connor, C. J.; Powell, G. L. *J. Am. Chem. Soc.* **1985**, *107*, 7438.
(23) Canich, J. M.; Cotton, F. A.; Daniels, L. M.; Lewis, D. B. *Inorg. Chem.* **1987**, *26*, 4046.
(24) Cotton, F. A.; Daniels, L. M.; Dunbar, K. R.; Falvello, L. R.; O'Connor, C. J.; Price, A. C. *Inorg. Chem.* **1991**, *30*, 2509.